

# Chapter 13

## High Harmonic Generation

High harmonic generation (HHG) is a technique for producing spatially and temporally coherent extreme-ultraviolet (EUV) light, as well as light pulses as short as hundred attoseconds (1 attosecond =  $10^{-18}$  seconds). To support pulses at such short duration light with a frequency higher than the inverse pulse duration is required corresponding to EUV wavelength of tenth of nanometers and shorter. Construction of lasers at these wavelengths is challenging and other means of producing significant EUV radiation, such as synchrotrons and Free-Electron Lasers (FELs) are rather expensive. HHG has the potential for generating significant coherent EUV radiation, even in the form of ultrashort pulses with attosecond duration opening up the new field of ultrafast x-ray spectroscopy.

HHG occurs when an intense pulsed laser beam is focused into a (noble) gas jet or solid. The intensity of the laser light is chosen such that its electric field amplitude is comparable to the electric field in atoms. Such fields are able to detach electrons from atoms by tunnel ionization, as opposed to photo-ionization by a weak field with high enough photon energy. The detached electron is accelerated in the field and under certain conditions has significant probability to hit the ion left behind upon return. The "collision" results in the emission of high energy photons. This description is called three step model and depicted in Figure 13.1

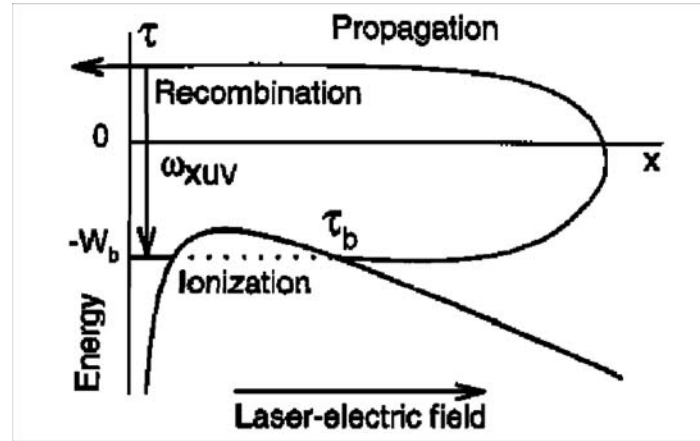


Figure 13.1: Three step model of High Order Harmonic Generation.

## 13.1 Atomic units

The dynamics of electrons in electric fields of atomic strength is most conveniently described in *atomic units*. Then typically atomic magnitudes are numbers of order one, which is very convenient. Atomic units are used in the vast majority of atomic physics literature, and in particular in the HHG literature.

In atomic units Planck's constant  $\hbar$ , the electron mass,  $m$ , and the electron charge,  $q$ , are set to one. Mass, charge and angular momentum are therefore measured relative to these magnitudes, and once three of them are given, the atomic unit for every other physical magnitude can be defined. In order to gain some intuition about atomic units, it is instructive to think about the Bohr hydrogen atom, with the electron moving around the proton in a circular orbit whose radius is the Bohr radius (see Fig. 13.2). Table 13.1 lists the definitions of some atomic units and conversion ratios to SI units:

For example, the hydrogen ionization energy is  $\frac{1}{2}\text{au}$ , and that of helium is about  $0.9\text{au}$ . Another example is the dielectric susceptibility of matter. Ignoring for the moment tensorial and non-instantaneous effects we can write for the polarization of a medium

$$P = \epsilon_0 (\chi^{(1)}E + \chi^{(2)}E^2 + \chi^{(3)}E^3 + \dots) \quad (13.1)$$

The nonlinear susceptibilities in SI units are of the order of  $10^{-12}$  for  $\chi^{(2)}$

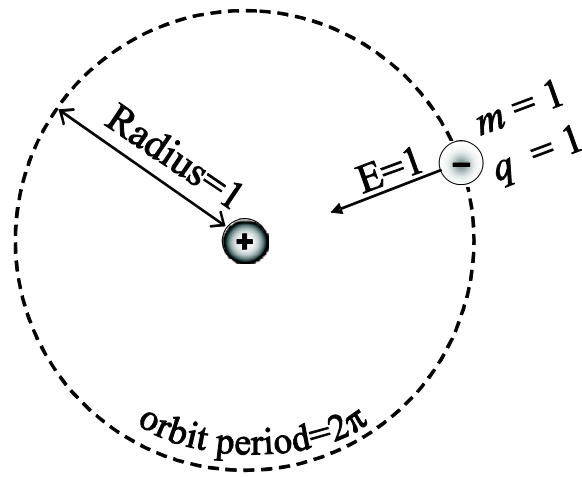


Figure 13.2: Definitions of atomic units through the Bohr model of the hydrogen atom.

and  $10^{-23}$  for  $\chi^{(3)}$ . When  $P$  and  $E$  are expressed in atomic units, all the  $\chi$ -s are of order one, because the electric field is then expressed in units of the electric field in an atom. We can argue that once the electric field reaches atomic fields, all harmonics of the fundamental laser wave will be observed, with intensities of similar orders of magnitude. Indeed HHG occurs only when such intensities are reached.

A typical field amplitude for HHG in helium is  $0.3 \text{ au} \approx 1.7 \times 10^9 \text{ V/cm}$ . The corresponding intensity is  $0.5 \cdot E^2/377\Omega \approx 4 \times 10^{15} \text{ W/cm}^2$ . For a Ti:sapphire beam (800 nm wavelength) focused to a  $25 \mu\text{m}^2$  spot and for a pulse duration of 10 fs we find that the pulses should carry about 0.1 mJ of energy.

## 13.2 The three step model

HHG photon energies achieved today reach up to 1.3 keV, which is about 50au. This high photon energy was achieved in helium. If we adopt the familiar picture (see Fig. 13.1), according to which a photon at certain energy is emitted when an electron “falls” from an excited state to the ground state, we see that the electron must “fall” from a very highly excited free state

Atomic unit of...	Definition	In SI units
Electric charge	The electron charge	$1.602 \times 10^{-19} \text{ C}$
Mass	The electron mass	$9.109 \times 10^{-31} \text{ kg}$
Length	The Bohr radius	$5.2917 \times 10^{-11} \text{ m}$
Time	$1/2\pi$ of the first Bohr orbit period	24.189 asec
Energy	The potential energy of the electron in the first Bohr orbit	27.21eV= $= 4.359 \times 10^{-18} \text{ J}$
Electric field	The electric field at the first Bohr orbit	$5.142 \times 10^{11} \text{ V/m}$

Table 13.1: Definitions of atomic units for some often used quantities and conversion to the SI system.

(50 times the binding energy). Since the potential is negative, high energy necessarily means high kinetic energy i. e. high velocity.

In order that a force of  $\sim 1 \text{ au}$  accelerates the electron to such high kinetic energy, it should travel a long distance away from the atom. According to the three step model, the electron is released from the atom by the laser field, accelerated in the free field away from the atom, then accelerated back towards the atom and collides with it. The energy lost in the collision shows up as a UV photon. The sequence of tunnel ionization, acceleration in the laser field and recollision is the called the three step model of HHG [2][3].

In order to estimate the energy acquired by the accelerating electron, we consider a free electron in a harmonic field of amplitude  $E$  and angular frequency  $\omega$ . The time-averaged kinetic energy equals

$$U_p = \left( \frac{qE}{2m\omega} \right)^2 = \left( \frac{E}{2\omega} \right)^2, \quad (13.2)$$

where the first expression is in general units ( $q$  is the electron charge) and the second one in atomic units. Note that this is a purely classical object since it does not involve  $\hbar$ .  $U_p$  is commonly referred to as the *ponderomotive energy*.

In order to achieve high ponderomotive energy,  $\omega$  must be a small number, that is, the optical frequency of the laser pulses must be much slower than atomic timescales.

### 13.2.1 Ionization

There are three regimes of ionization of an atom by an optical field. We consider here only fields of frequency  $\omega$  such that  $\omega < I_p$  ( $\hbar\omega < I_p$  in general units.  $I_p$  is the ionization potential of the atom). Therefore photoionization by a single photon is impossible.

#### 1. Multiphoton ionization.

This is the dominant regime for "small" fields, i.e. large Keldysh parameter  $\gamma = \sqrt{2I_p}/E > 1$ . It is characterized by a power law dependence of the ionization rate on the laser intensity, where the exponent is the minimal number of photons required for ionization (see Fig. 13.3). This regime is of less importance to HHG and we do not further discuss it here. The multiphoton regime takes place when  $E \ll 1\text{au}$  and  $U_p \ll I_p$ .

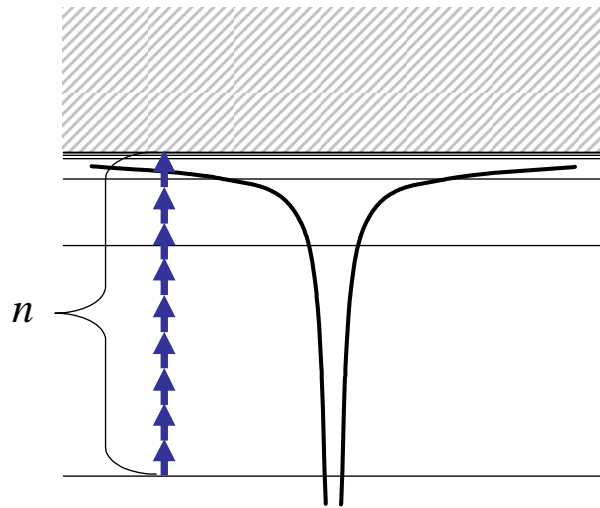


Figure 13.3: Ionization by  $n$  photons.

#### 2. Tunnelling regime.

Tunnelling is the dominant regime when  $U_p \gtrsim I_p$ , i.e.  $\gamma < 1$ , but  $E$  is small enough such that the barrier-suppression regime (the next one) is not yet reached, see Figure 13.4 and 13.5. The electron is released through tunnelling.

This regime is characterized by an exponential dependence of the ionization rate on the instantaneous electric field [4]:

$$w(E) \sim \exp\left(-\frac{2(2I_p)^{3/2}}{3E}\right), \quad (13.3)$$

where the ‘ $\sim$ ’ sign stands for "equal up to a sub-exponential factor in  $E$ ".

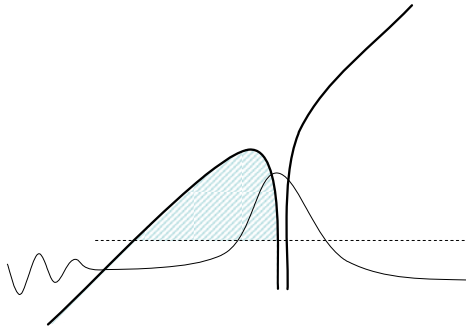


Figure 13.4: Ionization by tunnelling. The shaded area is the barrier, the classically forbidden region. The rate of tunnel ionization is exponential in the "area" under the barrier.

### 3. Barrier-suppression regime.

This regime is reached when the field is strong enough such that there is no energy barrier separating the electron from the free space (see Fig. 13.5). The barrier suppression regime is characterized by a nearly linear dependence of the ionization rate on the incident electric field.

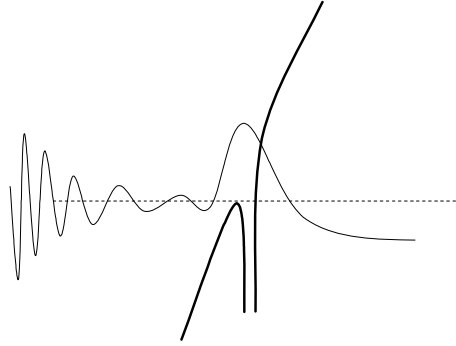


Figure 13.5: Ionization in the barrier-suppression regime.

When  $\omega \ll I_p$  the two last regimes are well described by the *quasi-static approximation*. The reason for this terminology is that the variation of the laser field is so slow that the instantaneous ionization rate coincides with a static one. Let then  $w(E)$  be the static ionization rate as function of the electric field. In the tunnelling and the barrier suppression regimes, with  $\omega \ll I_p$ , we therefore have

$$|a(t)|^2 = \exp \left( - \int_0^t w(E(t')) dt' \right), \quad (13.4)$$

where  $a(t)$  is the probability amplitude of finding the atom in the ground state. Note, that for  $\omega t \gg 1$  the ionization rate does not depend on  $\omega$ . This is in contrast with the multiphoton regime, where the rate exponentially decreases as  $\omega \rightarrow 0$ .

The static ionization rate  $w(E)$  is well described in the tunnelling regime by the Ammosov-Delone-Krainov formula [4]. For hydrogen and helium  $w(E)$  has been numerically calculated to high precision, and is shown in Fig. 13.6

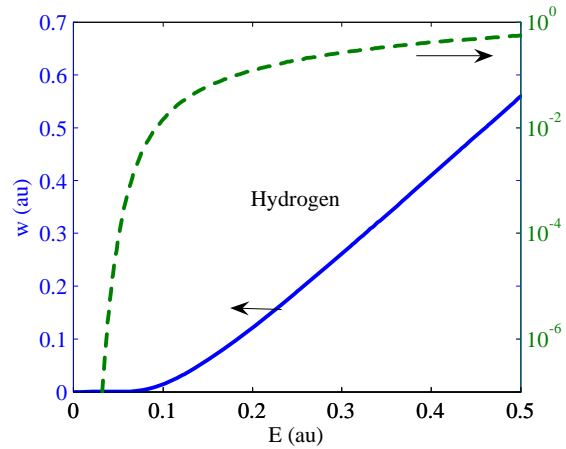


Figure 13.6: Static ionization rate for Hydrogen on a linear and logarithmic scale.

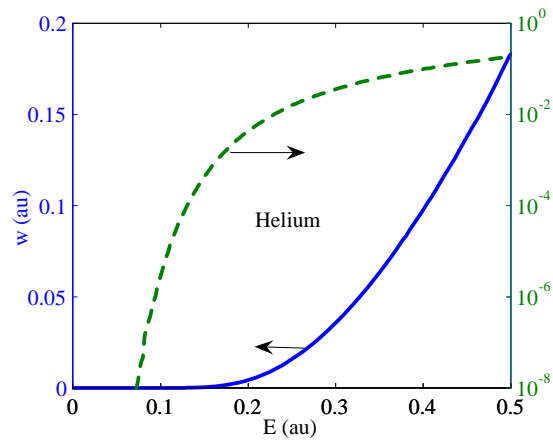


Figure 13.7: Static ionization rate for Helium on a linear and logarithmic scale..

### 13.2.2 Propagation

According to the correspondence principle, at high energies quantum mechanics should resemble classical mechanics. Indeed it turns out that the

propagation of the freed electron can be very well described classically. Since the Coulomb force exerted on the electron by the ion is negligible compared to the laser field during most of the electron excursion, the motion of the electron is well described by a free electron accelerated in the presence of the electric field of the laser pulse. Since we expect that the electrons do not reach relativistic speeds, we can neglect the Lorentz Force. It also turns out that the right after the tunneling, the velocity of the electron vanishes, i.e. the electron starts with zero velocity in the external field.

$$\ddot{x}(t) = E_0 \cos \omega t \quad (13.5)$$

$$\dot{x}(t) = \frac{E_0}{\omega} \sin \omega t - \frac{E_0}{\omega} \sin \omega t_0 \quad (13.6)$$

$$x(t) = -\frac{E_0}{\omega^2} \cos \omega t - (t - t_0) \frac{E_0}{\omega} \sin \omega t_0 + \frac{E_0}{\omega^2} \cos \omega t_0, \quad (13.7)$$

see Figure 13.8. Here,  $t_0$  is the time at which the electron was released from the atom. It is assumed that the electron is released with zero initial velocity. This assumption can be justified quantum mechanically. Since the electron is a quantum particle, it is released at all possible times  $t_0$  “together”. Each moment there is a probability amplitude to be released, depending (in the quasi-static approximation) on the electric field at that moment.

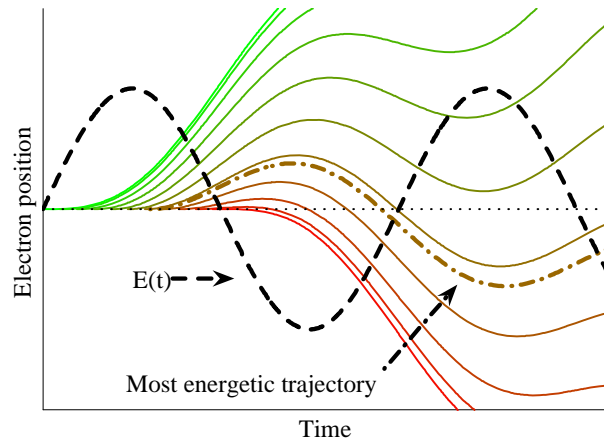


Figure 13.8: The position of the electron as function of time for different “ionization times”  $t_0$ . The “most energetic trajectory” refers to the solution where the electron encounters the nucleus with the maximal kinetic energy.

According to the three step model, the energy lost by the electron when it recollides with the nucleus is released as an HHG photon. We therefore wish to know how much kinetic energy the electron has when it returns. To this end we need to solve the Eq. (13.5) for  $x(t) = 0$  for some  $t$  and compute the kinetic energy  $\dot{x}^2(t)/2$  at that instant.

The solution cannot be expressed in terms of elementary functions. However, it can be easily found on a computer. It is easy to see that electrons re-encounter the nucleus only if they are released when the magnitude of the field is *decreasing* (see Fig. 13.8). The kinetic energy upon the first encounter of the electron with the nucleus is plotted in Fig. 13.9 as function of the ionization time  $t_0$ . It reaches a maximum for  $\omega t \approx 0.31$ , and the maximum approximately equals  $3.17U_p$ , which the ponderomotive energy  $U_p = \left(\frac{E}{2\omega}\right)^2$  of an electron in the laser field.

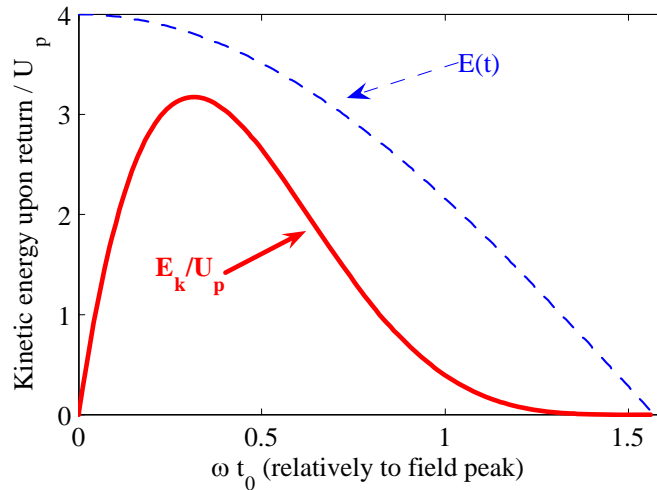


Figure 13.9: Kinetic energy upon return to the nucleus as function of the “ionization time”. The maximum is achieved about 0.31 radians after the peak of the electric field. For that case, the kinetic energy upon return reaches  $3.17U_p$ . The dashed curve is the electric field.

### 13.2.3 Recombination

A proper description of the recombination stage requires a quantum mechanical treatment of the rescattering problem and the emission of radiation. We

need to start from the Schroedinger equation of an electron bound to the atom, later partially tunneling ionized and accelerated. This is described by the Schroedinger equation of a single active electron in dipole approximation

$$i \frac{d}{dt} |\psi\rangle = H |\psi\rangle - E(t)x \quad (13.8)$$

with the atomic Hamiltonian

$$H = -\frac{1}{2}\nabla^2 + V(\vec{r}), \quad (13.9)$$

where,  $V(\vec{r})$  is the effective atomic potential confining the electron to the atom. Due to the interaction with the laser field we expect that the wavefunction of the electron, that is initially in the ground state  $|0\rangle$  with energy eigenvalue  $-I_P$ , where  $I_P$  is the ionization potential, evolves into a superposition state between the ground state with probability amplitude  $a(t)$  and a wavefunction describing the freed electron

$$|\psi(t)\rangle = a(t) |0\rangle + |\varphi(t)\rangle. \quad (13.10)$$

The freed electron together with the remaining ion forms a dipole and the expected value of the dipole moment is like for a two level system atom

$$\vec{d}(t) = \langle \psi(t) | \vec{x} | \psi(t) \rangle. \quad (13.11)$$

However, what acts as the source for electromagnetic radiation is not the dipole moment but rather the dipole acceleration. With the Ehrenfest Theorem in Quantum Mechanics, which is simply the Heisenberg equation of motion for the electrons kinetic momentum

$$\ddot{\vec{x}} = -\nabla V(\vec{r}) + E(t)\hat{x}. \quad (13.12)$$

and neglecting the external field coming from the laser, since it doesn't contain Harmonics, the dipole acceleration contributing to HHG can be written as

$$\ddot{\vec{d}}_{HHG}(t) = -\langle\psi(t)|\nabla V(\vec{r})|\psi(t)\rangle \quad (13.13)$$

$$= -|a(t)|^2\langle 0|\nabla V(\vec{r})|0\rangle - a(t)\langle\varphi(t)|\nabla V(\vec{r})|0\rangle \\ - a^*(t)\langle\psi(t)|\nabla V(\vec{r})|0\rangle - \langle\varphi(t)|\nabla V(\vec{r})|\varphi(t)\rangle. \quad (13.14)$$

$$\sim -a^*(t)\langle\varphi(t)|\nabla V(\vec{r})|0\rangle - a(t)\langle 0|\nabla V(\vec{r})|\varphi(t)\rangle \quad (13.15)$$

$$= \ddot{\xi}(t) + \ddot{\xi}^*(t), \text{ with } \ddot{\xi}(t) = -a^*(t)\langle\varphi(t)|\nabla V(\vec{r})|0\rangle \quad (13.16)$$

The first term vanishes, because of inversion symmetry of the atomic ground state and the last term is neglected, because it is expected to be small.

After some calculations, the result is [5]

$$\ddot{\xi}(t) = 2^{3/2}\pi(2I_p)^{1/4}e^{i\pi/4}\sum_n\frac{a(t_{nb}(t))a(t)\sqrt{w(Et_{nb}(t))}}{E(t_{nb}(t))(t-t_{nb}(t))^{3/2}}\vec{\alpha}_{rec}e^{-iS_n(t)}.$$

Here, the probability amplitudes of the ground state enter at the birthtime  $t_{nb}(t)$ , and  $t$ , if  $t$  is the recollision time of the trajectory. The recombination

matrix element  $\vec{\alpha}_{rec} = \langle k(t)|\nabla V(\vec{r})|0\rangle$  and  $S_n(t) = \frac{1}{2}\int_{t_{nb}(t)}^t k(t')^2 dt' + I_p(t - t_{nb}(t))$  is the classical action, the electron picks up during acceleration. The sum over  $n$  is the sum over all trajectories arriving at time  $t$ .

It is plausible that the energy released during recombination equals the kinetic energy the electron acquired plus the ionization potential, since the electron transitions from the continuum to a state with energy  $-I_p$ . In particular, we can expect the maximal energy released in the collision to be

$$\omega_{hmax} = I_p + 3.17U_p. \quad (13.17)$$

Figure 13.10 shows the Fourier transform of the calculated dipole acceleration for hydrogen excited by Ti:sapphire (800nm, corresponding to  $\omega = 0.057\text{au}$ ) pulses with an ideal sinusoidal single cycle pulse ( $E(t) = E_0 \sin \omega t$ ). The field amplitude used is shown near each spectrum. ( $\omega_{hmax} = I_p + 3.17U_p$  in atomic units). Remarkably Eq. (13.17), which is obtained from very simple considerations, gives the correct prediction for the cutoff of the spectrum. No harmonics above  $\omega_{hmax}$  are observed<sup>1</sup>, see Fig. 13.10. However, below the

<sup>1</sup>To be more precise, quantum mechanical analysis reveals that the cutoff formula  $\omega_{hmax} = 1.28I_p + 3.17U_p$ .

cutoff energy we observe oscillations in the high harmonic spectrum. This results from interference of contributions from the long and short trajectories, which contribute to the same frequency, energy, as can be seen from Fig. 13.8.

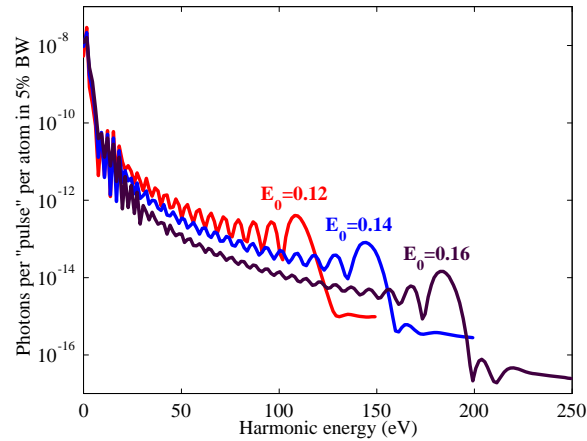


Figure 13.10: Simulated HHG spectra for hydrogen excited by Ti:sapphire (800nm, corresponding to  $\omega = 0.057\text{au}$ ) pulses with an ideal sinusoidal single cycle pulse ( $E(t) = E_0 \sin \omega t$ ). The field amplitude is denoted near each spectrum.

Figure 13.11 shows the kinetic energy normalized to the pondermotive potential that each trajectory contributes as a function of arrival time.

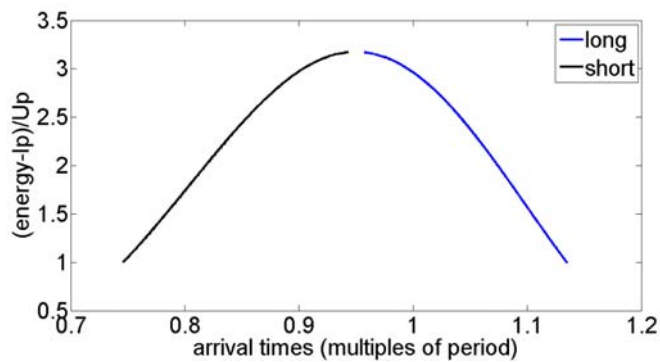


Figure 13.11: Kinetic Energy of long and short trajectories as a function of arrival time.

Figure 13.12 shows the Fourier transform of the calculated dipole acceleration for hydrogen excited by Ti:sapphire pulses with a secant hyperbolic pulse, 5fs FWHM duration and a maximal field amplitude of 0.12au. The spectrum is the cumulative effect of several cycles

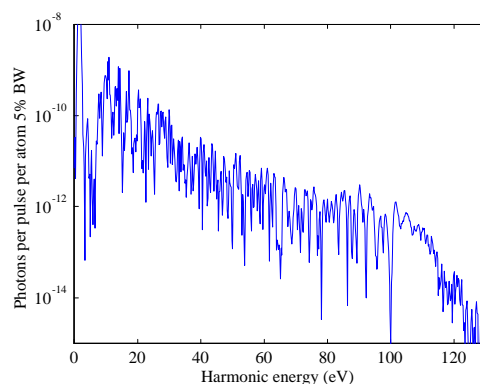


Figure 13.12: Simulated HHG spectra for hydrogen excited by Ti:sapphire (800nm, corresponding to  $\omega = 0.057\text{au}$ ) pulses with a secant hyperbolic pulse with 5fs FWHM duration and a maximal field amplitude of 0.12au.

The spectrum is the cumulative effect of several cycles, where in each half cycle a small fraction of the atoms are ionized, see Fig. fch13\_multicyclehgg

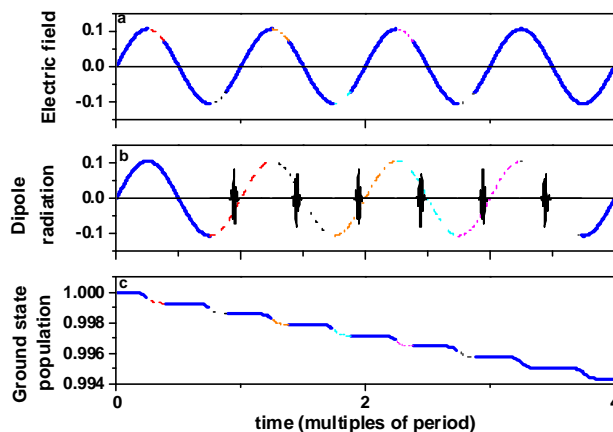


Figure 13.13: High harmonic generation dynamics in a multicycle pulse.

### 13.3 Attosecond pulses

The electron which acquires the largest amount of kinetic energy leaves the atom  $0.31\omega^{-1}$  after each peak of the field and hits the nucleus back at time  $4.4\omega^{-1}$  (about  $3/4$  of a cycle) after that peak (see Figs. 13.8, 13.14). Electrons that hit the nucleus later (short trajectories) or earlier (long trajectories) have less kinetic energy upon return. Thus the HHG radiation emitted by the recolliding electron has two contributions, one from the long and one from the short trajectories, both of which are down or up chirped (see Fig. 13.15).

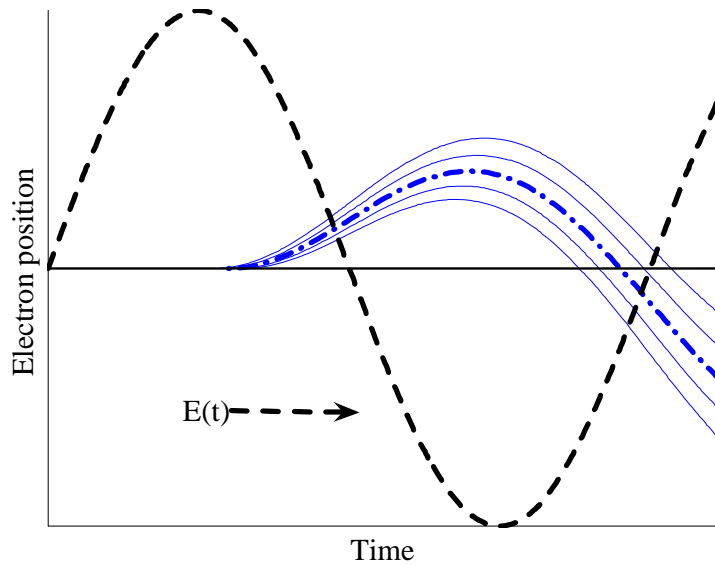


Figure 13.14: A single cycle, with a single recollision, leading to an isolated attosecond pulse. Most energetic trajectory (dash dotted line).

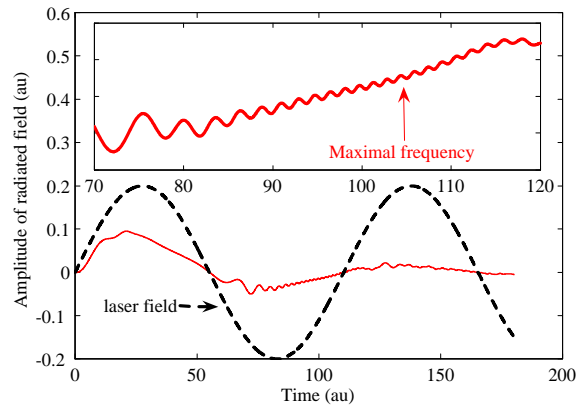


Figure 13.15: Neighborhood of the most energetic trajectory, which is responsible for the highest frequency radiation emitted.

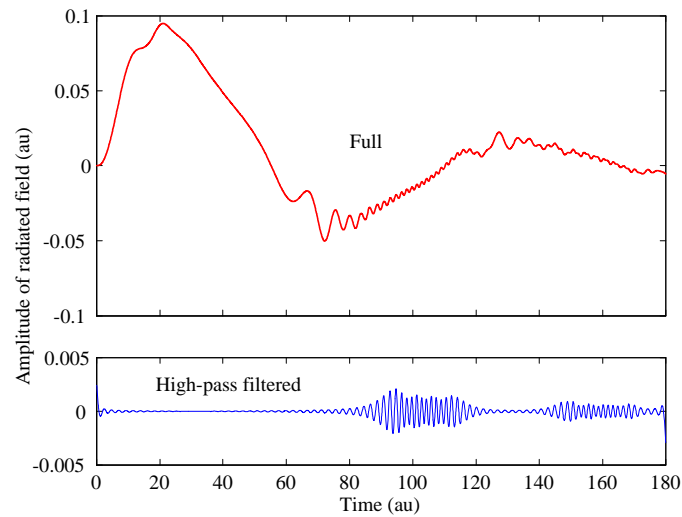


Figure 13.16: The same as Fig. 13.14a, before and after high-pass filtering.

There are several possibilities to select attosecond duration pulses, from this emission. First it was proposed to select isolated attosecond pulses, by using about two-cycle pulses and using high pass filtering of the emitted HHG

radiation to select the cut-off spectrum produced by the highest field cycle. Such a filtering is possible by using a multilayer MoSi-mirrors. Fig. 13.16 shows simulated electric field amplitude of the emitted HHG radiation before and after high-pass filtering. At the output of the filter we observe isolated pulses of several hundreds of attoseconds [7][9]. Other possibilities are to use polarization gating to achieve HHG in a single cycle from a few-cycle pulse and select the emission from the short or long trajectories and compression of these chirped emission using material dispersion in thin metal films [8]. The gating techniques have been further refined over the last years to a scheme called double-optical gating where both polarization and second harmonic field is used to further constrain HHG within a multicycle pulse.

### 13.3.1 The intensity challenge

HHG was discovered in 1987. Due to the progress in short pulse high energy Ti:sapphire lasers (30fs, 1mJ) it became possible to expose atoms to very high field strength before complete ionization and in 1997 EUV radiation down to 2.5 nm wavelength was demonstrated using HHG [6]. The shortest HHG wavelength demonstrated so far is 1nm (2005), however the efficiencies are very small at these short wavelengths.

### 13.3.2 The necessity of short drive pulses

Short pulses are a necessity for HHG in order to avoid depletion of the ground state during previous pulse maxima.

Fig. 13.17 shows the population of the ground state of Helium calculated with Eq. (13.4). When the pulses are not short enough (50fs in that particular example) most of the ground state is already depleted before the peak of the pulse is reached. Therefore the HHG radiation is released by electric fields of lower amplitude than the peak of the pulse, and most of the intensity of the pulse is "wasted".

The shorter the pulses become, the higher will be the ground state population when the atom experiences the peak of the electric field. Therefore short (few-cycle) pulses are a necessity for HHG, even when sufficient peak power is available.

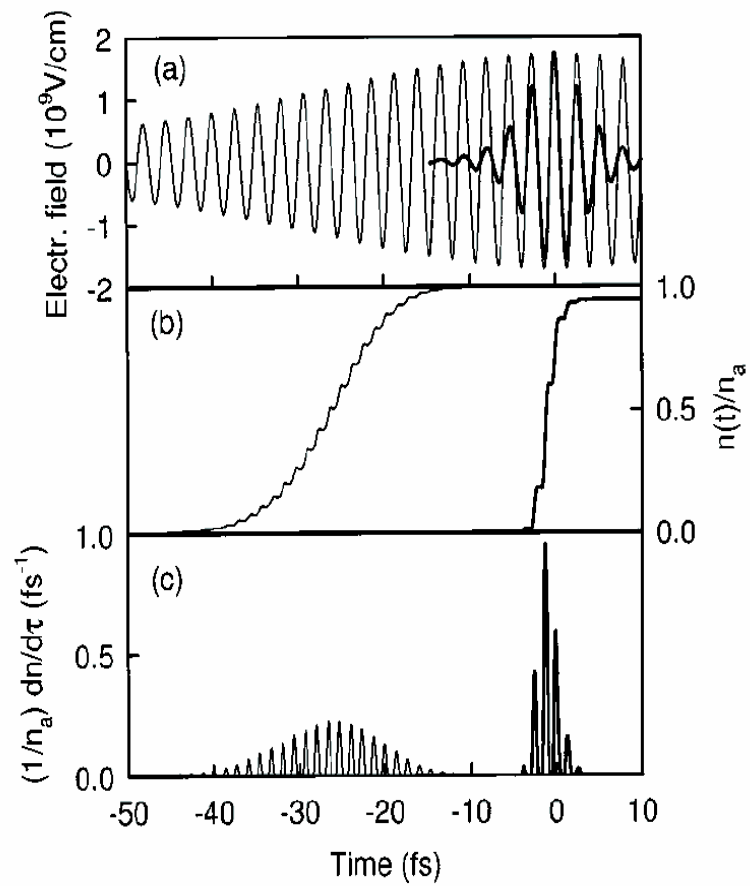


Figure 13.17: Ionization of helium in the presence of a linearly polarized electric field of a laser pulse with 800nm wavelength and a peak intensity  $4 \times 10^{15} \text{W/cm}^2$ : (a) electric field; (b) fraction of ionized electrons; (c) instantaneous ionization rate. The thin and the thick lines represent pulses of durations of 50fs and 5fs FWHM, respectively.[1]

### 13.3.3 Quantum diffusion

The simple classical picture of the propagation stage gives the correct cutoff law. However quantum mechanically the electron propagates along many trajectories at the same time. In particular, there is an uncertainty in the lateral initial velocity of the electron, and it therefore has returning electron wave packet has components that miss the nucleus.

The above described behavior is called quantum diffusion: free electron wavepackets expand as they propagate, just like a light pulse in a dispersive medium. The electron wavepacket expands as  $\sqrt{\tau}$  ( $\tau$  is the time of propagation between ionization and recombination) in each spatial direction. Therefore the amplitude in the center of the wavepacket decreases as  $\tau^{-3/2}$ . The amplitude of the emitted HHG electric field therefore scales like  $\tau^{-3/2}$ , and the intensity – like  $\tau^{-3}$ . The travel time is about an optical cycle.

The intensity of the HHG radiation therefore cubically decreases with increasing drive wavelength. However the spectral cutoff energy quadratically increases with it and the ionization of the atom can be reduced. The question what is the ideal drive wavelength to achieve maximum HHG for a desired wavelength range is not yet resolved.

### 13.3.4 Propagation effects – phase matching

In order to achieve efficient HHG, the contributions from single atoms emitting at different cycles and positions in the medium must interfere constructively with one another. Just like in second harmonic generation or optical parametric generation, phase matching is required. Phase matching is achieved, if the refractive index of the generated EUV radiation is equal to the index experienced by the driver laser pulse in the gas. The EUV radiation only weakly interacts with the gas and therefore propagates at the speed of light. However, the drive laser pulse experiences the dispersion from the gas, which increases the refractive index and the negative index of the free electrons generated (plasma). Choosing the proper ionization level and gas pressure is therefore important to achieve phase matching of the driver pulse and the generated EUV radiation.

Because of the phase mismatch and also because the spatial profile of the driver pulses, the pulse is distorted by the index profile of the free electrons, i.e. plasma defocusing of the laser beam occurs. Another limitation on the length comes from absorption: the longer the gas jet, the more it begins to

absorb the HHG photons. These effects severely limit the HHG conversion efficiency.

# Bibliography

- [1] T. Brabec and F. Krausz, "Intense few-cycle laser fields: Frontiers of nonlinear optics," *Rev. Mod. Phys.* **72**, 545-591 (2000).
- [2] P. B. Corkum, "Plasma Perspective on Strong-Field Multiphoton Ionization," *Phys. Rev. Lett.* **71**, 1994-1997 (1993).
- [3] M. Lewenstein, Ph. Balcou, M. Yu. Ivanov, A. L'Huillier, and P. B. Corkum, "Theory of High Harmonic Generation by low-frequency laser fields," *Phys. Rev. A.* **49**, 2117-2132 (1994).
- [4] M.V. Ammosov, N. B. Delone, and V. P. Krainov, *Sov. Phys. JETP* **64**, 1191 (1986).
- [5] A. Gordon and F. X. Kaertner, "Quantitative Modeling of Single Atom High Harmonic Generation," *PRL* **95**, 223901 (2005).
- [6] \bibitem{MurnaneScience98} A. Rundquist, C. G. Durfee, Z. H. Chang, C. Herne, S. Backus, M. M. Murnane, and H. C. Kapteyn, *Science* {\bf 280}, 1412 (1998).
- [7] M. Hentschel, R. Kienberger, C. Spielmann, G. A. Reider, N. Milosevic, T. Brabec, P. Corkum, U. Heinzmann, M. Drescher, and F. Krausz, "Attosecond metrology," *Nature*, vol. **414**, pp. 509-513, 2001.
- [8] G. Sansone, E. Benedetti, F. Calegari, C. Vozzi, L. Avaldi, R. Flammini, L. Poletto, P. Villoresi, C. Altucci, R. Velotta, S. Stagira, S. D. Silvestri, and M. Nisoli, "Isolated Single-Cycle Attosecond Pulses," *Science*, vol. **314**, pp. 443-446, 2006.

- [9] E. Goulielmakis, M. Schultze, M. Hofstetter, V. S. Yakovlev, J. Gagnon, M. Uiberacker, A. L. Aquila, E. M. Gullikson, D. T. Attwood, R. Kienberger, F. Krausz, and U. Kleineberg, "Single-Cycle Nonlinear Optics," *Science*, vol. **320**, pp. 1614 2008.